Sensors and Materials, Vol. 13, No. 7 (2001) 373–383
MYU Tokyo

S & M 0457

An Analytical Model for Passive Microvalves

Manuel Carmona, Santiago Marco, Josep Samitier,
María Cruz Acero[1], José Antonio Plaza[1] and Jaume Esteve[1]

Departament d'Electrònica, Associated Unit to the CNM-CSIC,
Universitat de Barcelona, C/ Martí Franquès 1, 08028-Barcelona, Spain
[1]Centre Nacional de Microelectrònica, Campus UAB, 08193-Bellaterra, Spain

(Received January 28, 2000; accepted August 7, 2001)

Key words: microvalve, modeling, VHDL-A, inviscid diffusion, wall shear, coupled problem, FEM.

An analytical model of a passive silicon microvalve of the bossed type has been extracted. This model involves three mathematical expressions that must be solved iteratively. They may easily be translated to an analog hardware description language. The main feature of this model consists of the inclusion of the diffuser effect. This effect is considerable at high *R*e and it has not usually been modeled in previous works. Comparison between the analytical model, FEM and experimental results shows good agreement, although some further improvements are required.

1. Introduction

Microvalves are a key component in most microfluidic applications. Passive ones have been fabricated for years[1–4] and they have been used in a multitude of different microdevices, mainly micropumps[5–8] or chemical analysis systems.[9] Nowadays, the modeling of a complex microdevice (such as a micropump) at a physical level is not practical. We must simplify the problem by splitting the device into minor components. A simplified model can be written using analog hardware description languages. To obtain a good model of a microdevice, accurate models for the different subcomponents are necessary. In many cases, realistic geometries do not permit simple analytical approaches, and numerical methods (such as the finite element method (FEM) or the finite difference method (FDM))

Corresponding author, e-mail address: santi@el.ub.es

are preferred. Often it is necessary to solve a coupled problem. For subcomponent models, it is convenient to use an iterative method (such as Gauss-Seidel or nested algorithms[10]) for the coupling process and one simulation algorithm for each physical domain. A suitable experimental setup for the measurement of the relevant characteristics is required for the validation and refinement of these models.

This work presents an analytical model for silicon passive microvalves (restricted to the bossed type), taking into account effects at the high flow regime (such as the diffuser effect, essential for nonlinear operation) and initial opening. The diffuser effect is related to the difference in pressure generated by a change in area through a fluidic channel. For a microvalve, this fact can be important; in this work we have a ratio of input to output areas up to 0.026, and this changes depending on the level of input pressure. As these microvalves are intended to operate with a thermo-pneumatic actuated micropump[11] (low-frequency operation), the conditions can be considered quasi-static in the mechanical and fluidic domains. Therefore, it is only necessary to extract a static model.

Three different designs have been microfabricated and modelled. The model predictions have been compared to FEM simulations and tested with filtered air.

2. Aspects of Microvalve Fabrication

A cross-section of the microvalve is shown in Fig. 1. It consists of a circular silicon mass suspended by two or four beams anchored on a Pyrex substrate. Inlet (or outlet) channels are drilled into this Pyrex substrate. The fabrication process for the microvalve is first a double step of reactive ion etching over a single crystal silicon bulk to define the anchor area of the microvalve and the arms, and the central mass. The etched distances determine the initial opening of the microvalve and the thickness of the arms and central

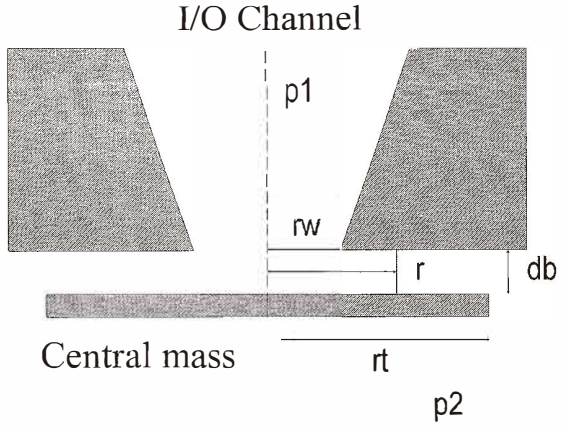

Fig. 1. Microvalve cross-section.

mass. The obtained silicon structure is anodically bonded through the anchor area to the Pyrex substrate. Finally, a deep tetramethylammonium hydroxide (TMAH) etch-back process releases the final structure. We have designed three different beams in order to obtain different rigidities. More details on the fabrication process can be found in ref. 12. Because of the fabrication process, the valves are initially open. The beams have a nominal thickness of 10 μm and a width of 50 μm, the initial opening is intended to be 2 μm, $r_t = 400$ μm and $r_w = 250$ μm. The length of the arms depends on the type of microvalve used, but it is about 1 mm. In Fig. 2, a scanning electron microscopy (SEM) image of a microvalve with two arms can be seen.

3. Microvalve Analytical Model

The microvalve model (Fig. 1) assumes axisymmetry and takes into account three effects: viscous wall shear, inviscid ideal diffusion and input nozzle resistance. The first effect is usually modeled and becomes relevant for low fluid flows. The remaining effects are usually neglected, but they must be considered for high fluid flows. The distribution of pressure over the central mass is given by:[13,14]

$$\frac{p(r)-p_2}{\rho \bar{U}^2/2} = 24\frac{r_w/d_b}{N_{R(d_b)}}\ln\left(\frac{r_t}{r}\right)+\beta_{et}\left(\frac{r_w}{r_t}\right)^2-\beta_e\left(\frac{r_w}{r}\right)^2,$$

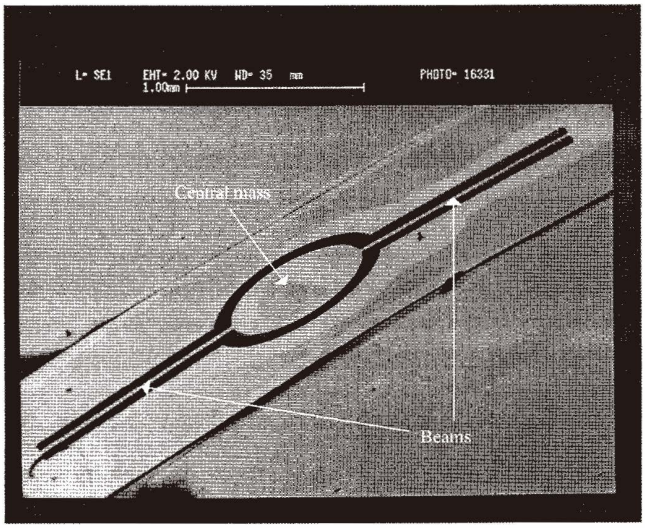

Fig. 2. SEM image of a microvalve with two arms.

where ρ is the density of the fluid, β_e is the energy distribution factor between parallel plates (equal to 1.543 for fully developed flow), $N_{R(db)}$ is the Reynolds number at the valve entrance ($r = r_w$), U is the mean velocity at $r = r_w$, p_2 is the output pressure, d_b is the opening of the microvalve, r_w is the radius of the input channel and r_t is the radius of the central mass. See Fig. 1 for the interpretation of the geometrical parameters.

The first term on the right-hand side is due to the wall shear effect (viscous losses along the channel), and the last two terms correspond to the ideal diffusion effect at the channel. This last effect becomes higher as the flow increases.

From the previous expression we can obtain the mean pressure over the valve lid. We have taken a constant pressure, equal to the input pressure, at the portion of the central mass out of the channel ($0 \le r \le r_w$). The new pressure distribution modifies the position of the central mass, modifying again the flow and pressure distribution. The new position is calculated from the mechanical relation between the displacement (Δz_{max}) and the mean pressure (ΔP) applied over the valve lid:

$$\Delta z_{max} = K^{-1} \cdot \Delta P,$$

The value of K can be obtained in two different ways:

–Analytical expression: Taking into account the expression for a clamped beam and guided end, K can be obtained from the following expression:

$$K = \left(\frac{\Delta z_{max}}{P_i} \right)^{-1} = n \cdot E \cdot b \left(\frac{h}{L} \right)^3 \frac{2 \cdot \ln\left(\frac{r_t}{r_w} \right)}{\pi \cdot \left(r_t^2 - r_t^2 \right)},$$

where P_i is the input pressure, K is the rigidity of the valve, n is the number of arms, h the thickness, b the width, L the length and E the Young's modulus.[15]

–Numerical methods: The main advantage is that we can consider the nonlinear relation between these two variables. Moreover, they permit us to take into account different boundary conditions.

Therefore, we have a problem that must be solved using an iterative method. We have applied the Gauss method and we have neglected the input nozzle effect that may cause a pressure transition at the entrance of the valve channel. Now, we need the apparent loss coefficient for the nozzle-valve structure that is obtained from the following expression:

$$K_A = 24 \frac{r_w / d_b}{N_{R(d_b)}} \ln\left(\frac{r_t}{r_t} \right) + \beta_c * \left(\frac{2 * db}{r_w} \right)^2,$$

where β_c is the energy distribution in a circular tube ($\beta_c = 2.0$). The first term on the right-hand side is the pressure loss due to wall shear in the region $r_w < r < r_t$, the second term is

the pressure loss due to the diffuser effect in the same region and the third one is due to the diffuser effect between the entrance and $r = r_w$.

This analytical model has been compared to previously published models, for example:[4]

$$Eu^4 \cdot N_R = \frac{96}{\pi^4} \cdot \Pi^3{}_{stiff} \cdot \frac{(\ln \Pi_{geom})^4}{(\Pi^2{}_{geom} - 1)^3},$$

to see the effect of taking into account the diffuser effect. Eu is the Euler number, N_R is the Reynolds number, Π_{stiff} is the dimensionless stiffness and Π_{stiff} is the ratio between the input and output radii. A comparison of flow-pressure characteristics between both models can be seen in Fig. 3. The difference appears to be significant at high flow rates. These pressure values are easily attainable in microfluidics applications.

By means of FEM simulations, we have obtained the pressure profile along the channel. A comparison of the pressure distribution with the predictions of the analytical model is shown in Fig. 4, which shows good agreement at low pressures. At high pressures, fully developed flow at $r_w = 250$ μm does not exist; this is shown in the figure by the lack of recovery of the pressure. However, such pressure levels are hardly achieved in our case due to the low rigidity of the valve. In Fig. 5, we see the valve center deflection obtained from FEM compared to the analytical model. As arm thickness is about 10 μm, for displacements on the same order of magnitude a nonlinear displacement-pressure characteristic of the valve should be taken into account. Furthermore, the same effects as previously discussed on the fluidic domain influence its response.

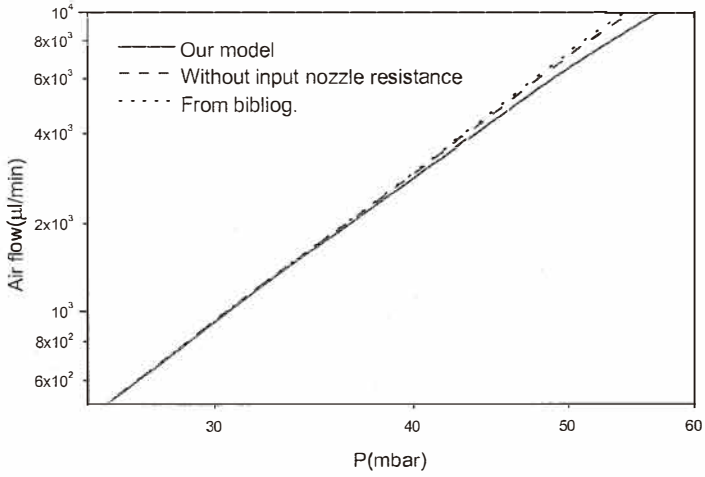

Fig. 3. Flow-pressure comparison between our model and a previous analytical model.

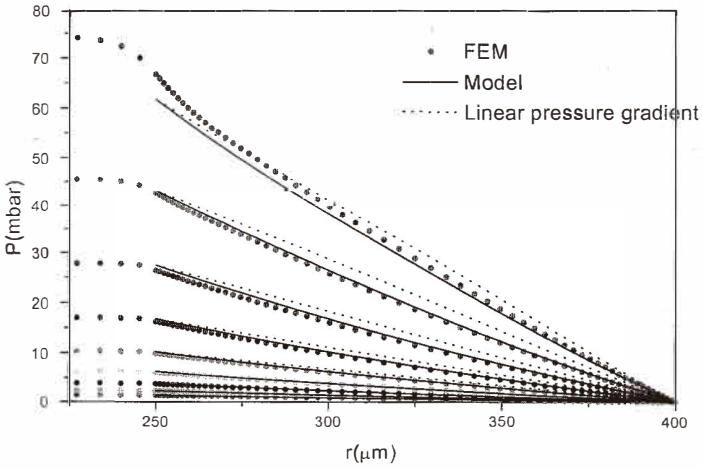

Fig. 4. Pressure distribution over the central mass obtained from FEM and the analytical model.

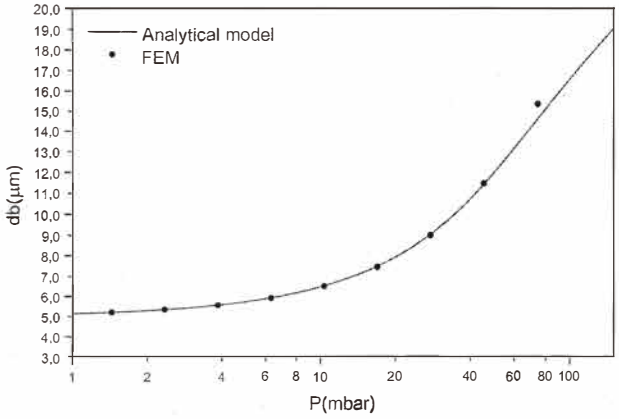

Fig. 5. Central displacement of the microvalve.

4. Comparison between FEM and the Analytical Model

First, we compared the rigidity of the microvalves with two arms obtained by both methods. We assumed a uniform pressure over the valve lid. The parameters are: $L = 1225$ μm, $h = 10$ μm, b=50 μm, $r_t = 400$ μm, $r_w = 250$ μm, $n = 2$. A comparison of the $\Delta z(P)$ characteristics for the FEM and analytical models is shown in Fig. 6. It can be seen that they agree at low mean pressures, but nonlinearities begin for pressures higher than 1 mbar.

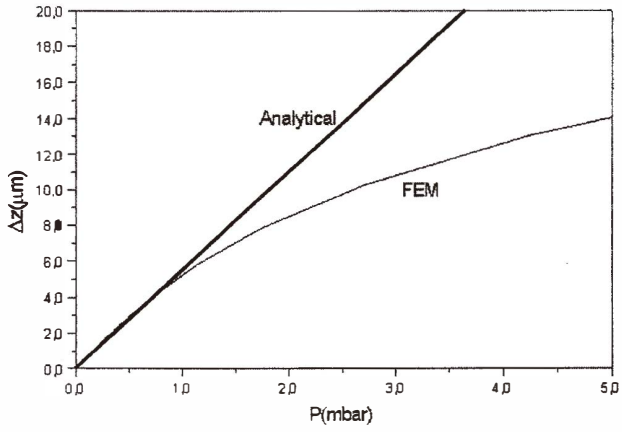

Fig. 6. $\Delta z/\Delta P$ extracted from analytical and FEM models.

The FEM simulations can also be used in the fluidic domain to compare results with the previous analytical model. FLOTRAN (ANSYS, Inc.) has been used with an axisymmetrical model (a centered inlet hole is assumed in simulations). The microvalve stiffness is assumed constant; only linear behaviour is considered. Due to the coupled problem of fluid structure, iterative FEM simulations were needed to obtain the flow-pressure characteristic. Turbulent flow (k-ε turbulence model) was considered at high pressures, but the results showed no difference with respect to laminar flow. The axisymmetric FEM model is shown in Fig. 7. A comparison of the flow-pressure characteristic with the model is shown in Fig. 8(a). There is a good agreement between them. First, we have a proportional relation between flow and pressure which is due to the initial opening of the microvalve; the central mass remains in the same position. Viscous losses are the dominant processes in this region. As the valve opens, the slope grows due to the valve opening and the diffuser effect must be taken into account. Divergences at high flow rates may be explained by several effects. The first one is that, as the opening increases, the flow cannot fully develop at the entrance of the channel, which modifies the β value in this region. Another effect is the existence of a pressure transition between the external pressure and the pressure at the channel entrance that we have not taken into account. This latter effect can also influence the β value. The microvalve has a large opening compared with the length channel at a high N_R. As all of these effects influence the parameter β, we have introduced a proportionality constant for this parameter, determined by least squares at high pressures. In Fig. 8(b), the results obtained by diminishing the inertial effects by a factor of 5 are shown. As can be seen, the simulations agree with model predictions at high pressures.

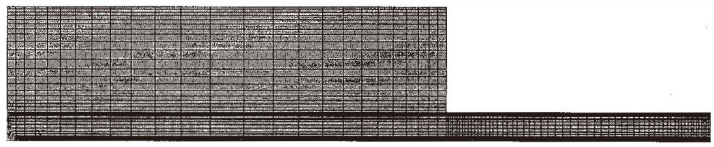

Fig. 7. FEM axisymmetric model.

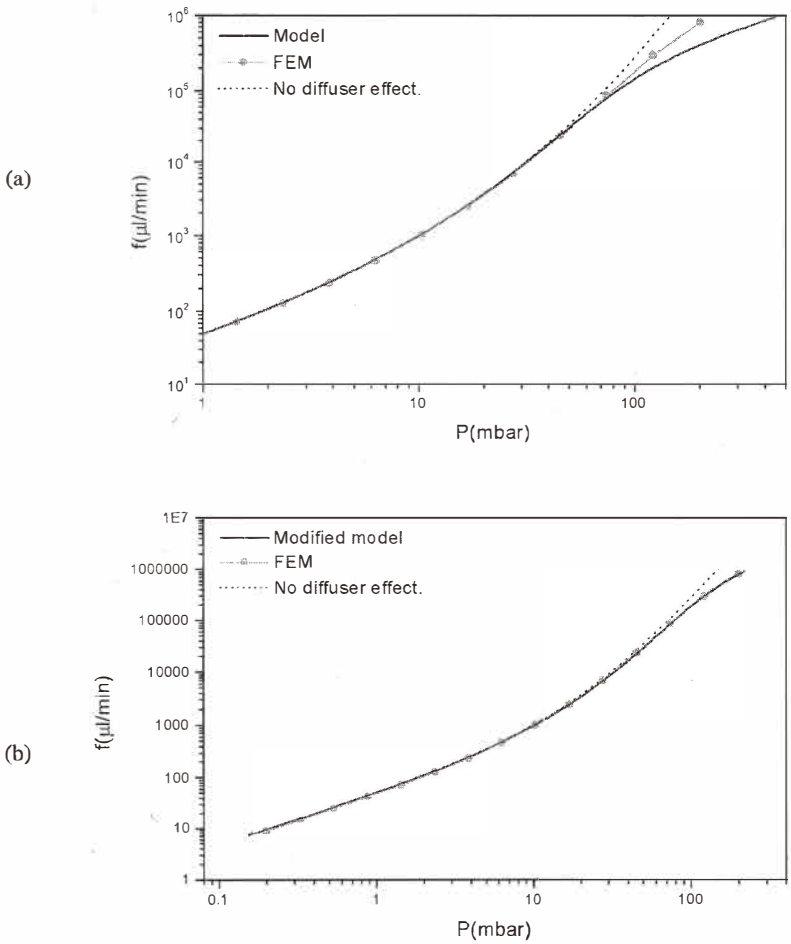

Fig. 8. Comparison of the flow-pressure characteristic between (a) FEM and the model and (b) with a modified model.

5. Flow Measurements and Model Validation

The flow-pressure characteristic has been measured with air. A schematic view of the experimental setup is shown in Fig. 9. A chamber is continuously filled with air by a peristaltic pump to achieve a certain pressure value at the entrance of the microvalve. At the moment this pressure value is achieved, we stop the input flow and the pressure decays slowly due to losses through the microvalve. This pressure transient is measured by a highly sensitive pressure sensor.

The air flow rate through the microvalve can be calculated from the measured pressure transient. If we approximate air as an ideal gas (a good approximation in this case because the increase in pressure with respect to atmospheric pressure is quite low) and assume a quasi-static state of the air (achieved using a high volume in the pre-chamber), the flow rate can be easily obtained by:

$$\phi_V = -\frac{R \cdot T_0}{M \cdot V}\frac{dP}{dt},$$

where ϕ_v is the volume flow, R is the gas constant, T the absolute temperature, V the volume of the chamber and M the mass of 1 mol of air.

The pressure transient is measured by a data acquisition board installed in a PC. The differentiation of the transient causes an amplification of the noise due to the high pass character of this signal processing operation. To avoid this problem, we have fitted the pressure transient using the sum of two decreasing exponentials. Figure 10(a) shows one of the experimental pressure transients obtained and Fig. 10(b), the extracted flow-pressure characteristic.

The initial opening and the spring constant of the microvalves can be extracted by fitting the measured values as shown in Fig. 10(b). The initial opening obtained for the three valves is about 5.5 μm. The value obtained by profilometer measurements is about 4 – 5 μm. There is a slight disagreement regarding this point. One interpretation of this result is the possible presence of a slip boundary condition at the plates along the channel; this effect can appear for channel widths of several microns.[16] This implies a lower flow

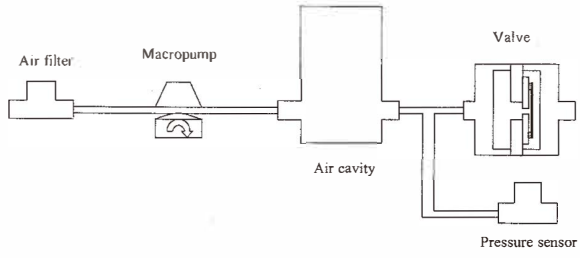

Fig. 9. Measurement setup.

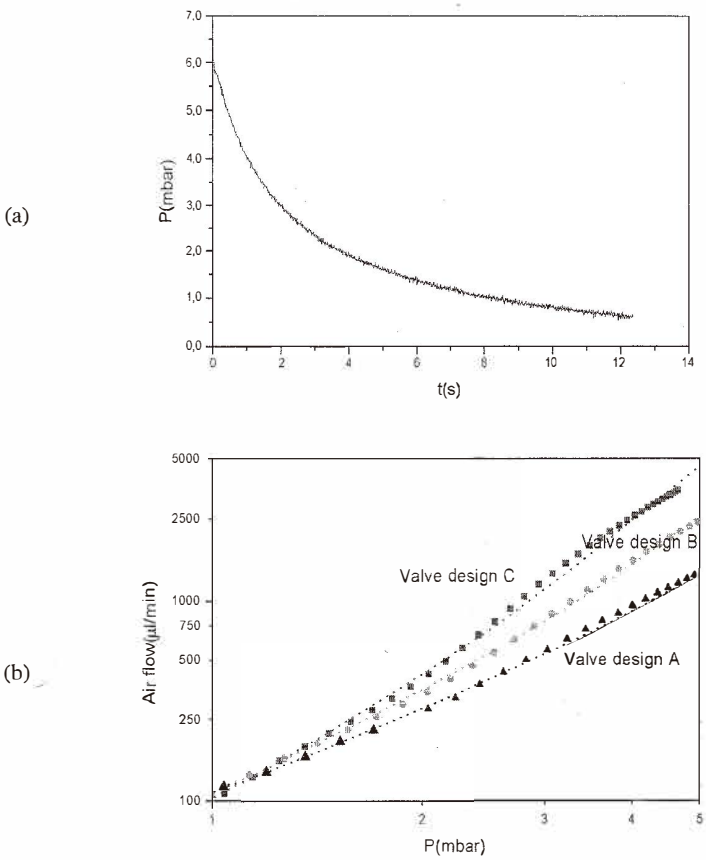

Fig. 10. (a) Measured pressure transient and (b) fitted flow-P results for three different designs.

resistance than that given by the analytical model and it was interpreted as a larger initial opening. In microfluidics, the importance of taking into account this effect when having air as the object fluid is well known[17,18]. In our case, the Knudsen number for small displacements of the microvalve is $Kn = 0.013$. It is within the slip flow condition. From results in the literature[17] for a rectangular channel, a Knudsen number of 0.015 and a Reynolds number of 50, we can obtain an error from a continuum consideration of less than 10%. The appreciated difference in the results mentioned before is well within this range.

The beam stiffness has been also determined by IR interferometry. The thickness of the arms measured by a profilometer is roughly 15 μm, significantly different from the technologically expected value of 10 μm. That means that we have stiffer structures. However, the arm thickness extracted from the experimental characteristics is nearly 15 μm and agrees well with the measured one.

6. Conclusions

We have presented an analytical model of a passive silicon microvalve (bossed type) characterised by an initial opening and including the ideal diffusion effect. This model has been validated with experimental measurements and FEM simulations, showing some discrepancies at high flow rates. The model has been corrected to take into account non-ideal effects, such as non-developed flow and pressure transitions at the entrance of the nozzle. Slip-boundary conditions should be considered for low pressures, as well as the mechanical nonlinear characteristic of the microvalve for high pressures.

References

1 M. Esashi, S. Shoji and A. Nakano: Sensors & Actuators A **20** (1989) 163.
2 M. Freygang, H. Glosch, H. Haffner, S. Messner, B. Schmidt and H. Straatman: ACTUATOR'94 p. 100.
3 W. K. Schomburg and B. Scherrer: Journal of Micromechanics & Microengineering **2** (1992) 184.
4 R. E. Oosterbroek, S. Schlautmann, J. W. Berenschot, T. S. J. Lammerink, A. van den Berg and M. C. Elwenspoek: Proceedings of the 1998 International Conference on Modelling and Simulation of Microsystems Semiconductors, Sensors and Actuators p. 528.
5 H. T. G. van Lintel, F. C. M van de Pol and S. Bouwstra: Sensors & Actuators A **15** (1988) 153.
6 J. G. Smits: Sensors & Actuators A **21–23** (1990) 203.
7 T. Gerlach and H. Wurmus: MEMS'95 221.
8 A. Olsson, O. Larsson, J. Holm, L. Lundbladh, O. Öhman and G. Stemme: Sensors & Actuators A **64** (1998) 63.
9 S. Shoji, S. Nakagawa and M. Esashi: Sensors & Actuators A **21–23** (1990) 189.
10 S. Schulte, A. Maurer and H. Bungartz: Modular solution approach for simulation of coupled physical phenomena, MicroSim, Ed. Computational Mechanics Publications (Southampton, 1995) p. 201.
11 M. C. Acero, J. A. Plaza, J. Esteve, M. Carmona, S. Marco and J. Samitier: Journal of Micromechanics and Microengineering **7** (1997) 179.
12 M. C. Acero: Tecnologóas de micromecanización y su aplicación a la fabricación de componentes para microfluídica, PhD Thesis, Centre Nacional de Microelectrònica, Bellaterra, Barcelona, 1998.
13 L. A. Zalmanzon: Components for Pneumatic Control Instruments (Pergamon, Oxford, 1965).
14 P. S. Moller: The Aeronautical Quarterly **14** 163.
15 J. Prescott: Applied elasticity (Dover Publications, Inc. 1961).
16 A. Beskok, G. E. Karniadakis and W. Trimmer: Journal of Fluids Engineering **118** (1996) 448.
17 A. Beskok and G. E. Karniadakis: DSC **40** (1992) 355.
18 E. B. Arkilic, M. A. Schmidt and K. S. Breuer: J of Microelectromechanical Systems **6** (1997) 167.